BULETINUL Universităţii Petrol – Gaze din Ploieşti	Vol. LXVII No. 2/2015	11 – 20	Seria Tehnică

Numerical Modelling of Damage and Failure of Ductile Materials in Finite Element Analysis

Dan Andrei Şerban[*,**], Emanoil Linul[*], Cristian Neş[*], Liviu Marşavina[*]

* Department of Strength of Materials, Politehnica University of Timisoara, Bd. M. Viteazu, 1, Timisoara
** Research Institute for Renewable Energy, Politehnica University of Timisoara, Str. G. Musicescu, 138
e-mail: dan.serban@upt.ro

Abstract

This work presents the main numerical models used in the simulation of damage and failure of ductile materials that are implemented in commercial software packages: equivalent strains criterion, shear criterion and the FLD criterion. Several numerical simulations were performed for impact loadings using one of the above mentioned degradation criteria as well as all criteria, in order to highlight the interaction between the models.

Key words: *finite element analysis, damage, failure.*

Introduction

The emergence of cracks in materials is a result of several complex physical processes that occur at a microstructural level. Fracture mechanics deals with the propagation of cracks in materials starting from pre-existing defects and flaws in the material.

At a macro scale, the parameters that appear to cause the failure of materials are the components of the stress and of the deformation tensors, the strain rate and the temperature [1, 2].

In this work, the main damage initiation criteria for ductile materials will be presented. Some commercial finite element analysis packages (Abaqus, LS-Dyna, PAM-Crash) have implemented these models into their code, and, if rightly calibrated, they can predict the damage and failure of various complex structures subjected to both static and dynamic loadings [3, 4].

The simulations presented in this study were performed in the commercial software Abaqus, using a constitutive model for an aluminium alloy as a material in order to illustrate the effects of the degradation models.

Overview of Macro-scale Modelling of Ductile Damage

The modelling of damage at a macro scale in finite element analysis software is achieved by reducing the stiffness of an element when a damage initiation criterion is met and eventually deleting the element when its rigidity reaches 0 as a consequence of a damage evolution law, as expressed in equation (1) and depicted graphically in Figure 1:

$$\boldsymbol{\sigma} = (1-d)\boldsymbol{D}_0^{el} : \left(\boldsymbol{\varepsilon} - \boldsymbol{\varepsilon}_{pl}\right) \tag{1}$$

where **1** is the Cauchy stress tensor, $\boldsymbol{D}_0^{el}$ represents the elasticity tensor, $\boldsymbol{\varepsilon}$ is the total strain tensor, $\boldsymbol{\varepsilon}_{pl}$ represents the plastic strain tensor while d represents a degradation factor. In Figure 1, the interval [0-A) on the stress-strain curve represents linear elasticity, {A} corresponds to the yield point and (A-B-C) is characterized by the material hardening. In case a damage initiation criterion is met at point {B}, the material's stiffness starts to decrease until it reaches 0 and the material fails.

As equation (1) shows, the degradation laws are dependent on material plasticity. Most implemented damage initiation criteria are compatible with the main plasticity models used in finite element analysis (von Mises, Johnson-Cook, Hill or Drucker-Prager) [5].

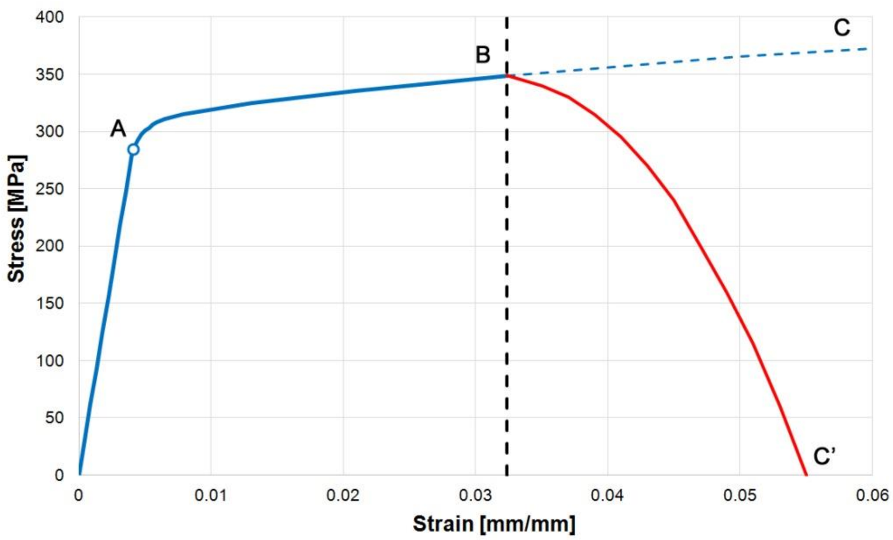

Fig. 1. Generic damage initiation and evolution

Damage Initiation Mechanisms

The damage imitation criteria presented in this paper were developed after observations of failure modes of ductile materials subjected to various loads.

Equivalent strains criterion

The equivalent strains criterion is based on the process of occurrence, growth and coalescence of voids in the deformed material [5]. In this case, the decrease in material stiffness (according to equation 1) is due to the reduction of the cross-section (figure 2).

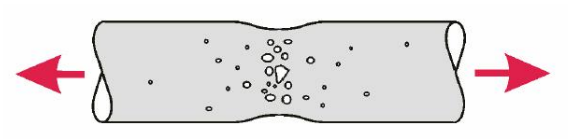

Fig. 2. Nucleation of voids during loading

Similar to the von Mises equivalent stress, the equivalent plastic strain is calculated with equation (2) [6]:

$$\varepsilon^{pl} = \sqrt{\frac{2}{3}\overline{\varepsilon^{pl}}:\overline{\varepsilon^{pl}}} \tag{2}$$

where $\overline{\boldsymbol{\varepsilon}^{pl}}$ represents the deviatoric (distortional) component of the plastic strain tensor $\boldsymbol{\varepsilon}^{pl}$ and it is obtained with the help of equation (3):

$$\overline{\boldsymbol{\varepsilon}^{pl}} = \boldsymbol{\varepsilon}^{pl} - \frac{1}{3}\mathrm{tr}\left(\boldsymbol{\varepsilon}^{pl}\right) \tag{3}$$

The equivalent plastic strain can be expressed as a function of the principal strains using equation (4):

$$\varepsilon^{pl} = \sqrt{\frac{3}{2}\left[\left(\varepsilon_1^{pl} - \varepsilon_2^{pl}\right)^2 + \left(\varepsilon_2^{pl} - \varepsilon_3^{pl}\right)^2 + \left(\varepsilon_3^{pl} - \varepsilon_1^{pl}\right)^2\right]} \tag{4}$$

where $\varepsilon_1^{pl}, \varepsilon_2^{pl}, \varepsilon_3^{pl}$ represent the principal plastic strains.

Thus, according to this criterion, the damage is initiated when the equivalent plastic deformation reaches a critical value $\varepsilon^{pl} = \varepsilon_D^{pl}$. The critical plastic deformation for initiating damage according to this criterion is a function of the triaxial state of stress and the strain rate [7, 8].

The triaxial state of stress η is defined as the hydrostatic pressure (or the mean stress) denoted with σ_m divided by the equivalent von Mises stress, denoted with $\bar{\sigma}$ [9]. This parameter was introduced in evaluating the failure of ductile materials after its large role in influencing critical strains was observed [10, 11, 12]. The formulas used in calculating he hydrostatic pressure and the equivalent von Mises stress are presented in equations (5 a) and (5 b).

$$\sigma_m = \frac{1}{3}(\sigma_{11} + \sigma_{22} + \sigma_{33}) \tag{5 a}$$

$$\bar{\sigma} = \sqrt{\frac{2}{3}\boldsymbol{\bar{\sigma}}:\boldsymbol{\bar{\sigma}}} = \sqrt{\frac{1}{2}[(\sigma_1 - \sigma_2)^2 + (\sigma_2 - \sigma_3)^2 + (\sigma_3 - \sigma_1)^2]} \tag{5 b}$$

In the case of finite element analysis, the equivalent plastic strains damage initiation criterion is reached when the relation form equation (6) is satisfied.

An example of the variation of the critical plastic strain with the stress triaxiality is presented in Figure 3 for the aluminium alloy EN AW-7108 T6 for both static and dynamic loads [13].

$$\omega_D = \int \frac{\mathrm{d}\varepsilon^{pl}}{\mathrm{d}\varepsilon_D^{pl}(\eta, \dot{\varepsilon}^{pl})} = 1 \tag{6}$$

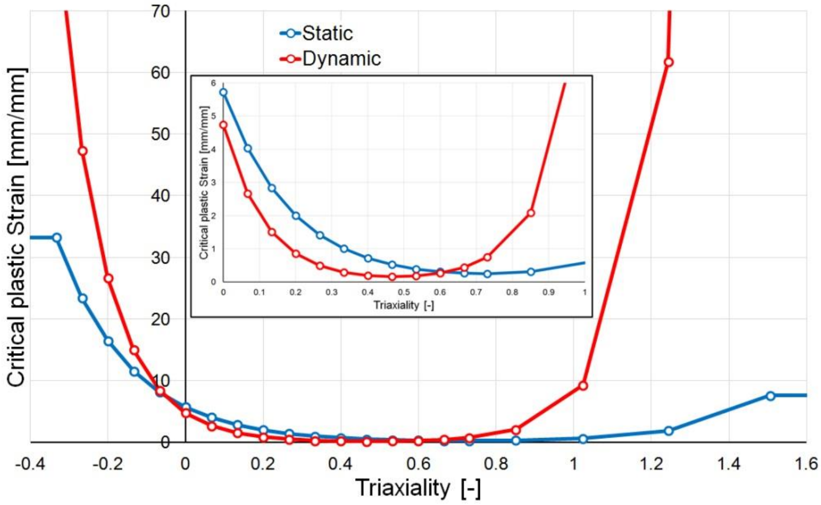

Fig. 3. Variation of the critical plastic strain with stress triaxiality for the EN AW-7108 T6 aluminium alloy

Shear criterion

The shear damage initiation criterion is based on the degradation of materials due to the occurrence of shear bands during loading (figure 4) [6, 14].

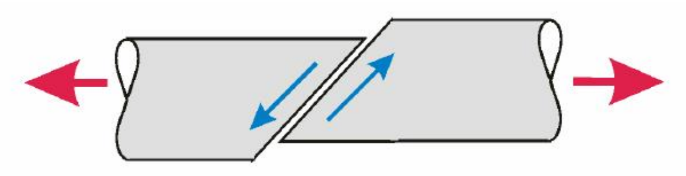

Fig. 4. Occurrence of shear bands during loading

In this criterion, the critical equivalent plastic strain ε_S^{pl}} is considered to be a function of the shear stress ratio θ_s and the plastic strain rate $\dot{\varepsilon}^{pl}$. The parameter shear stress ratio introduced in this formulation is a scalar value that is dependent on the equivalent von Mises stress $\bar{\sigma}$, the mean stress σ_m, the maximum shear stress τ_{max} and on a material parameter k, according to equation (7).

$$\theta_s = \frac{\bar{\sigma} + k \cdot \sigma_m}{\tau_{max}} \tag{7}$$

In a similar fashion to the equivalent strains criterion, the shear damage initiation criterion is reached when the relation form equation (8) is satisfied.

$$\omega_D = \int \frac{d\varepsilon^{pl}}{d\varepsilon_S^{pl}(\theta_s, \dot{\varepsilon}^{pl})} = 1 \tag{8}$$

An example of the variation of the critical plastic strain with the shear stress ratio is presented in Figure 5 for the aluminium alloy EN AW-7108 T6 for both static and dynamic loads [13].

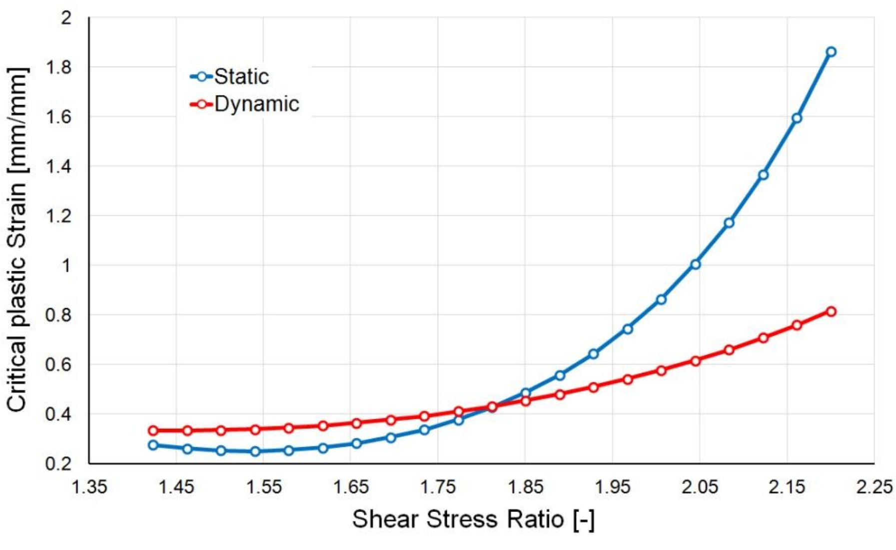

Fig. 5. Variation of the critical plastic strain with shear stress ratio for the EN AW-7108 T6 aluminium alloy

The Forming Limit Diagram (FLD) criterion

The Forming Limit Diagram was developed for the purpose of studying the amount of deformation a material can withstand before the onset of necking instability during sheet metal forming [14] (figure 6).

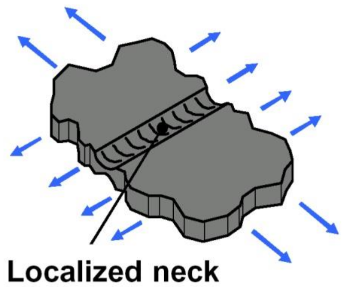

Fig. 6. Occurrence of necking during sheet metal loading

The forming limit diagram consists of a plot of the forming limit strains (maximum strains a sheet material can sustain prior to necking) in the space of principal logarithmic strains. The function representing the major principal strain as a function of the minor principal strain at the onset of damage represents the input data required for the calibration of the FLD criterion. This damage initiation criterion is achieved when equation (9) is satisfied.

$$\omega_D = \frac{\varepsilon_{\text{major}}}{\varepsilon_{\text{major}}^{FLD}(\varepsilon_{\text{minor}})} = 1 \tag{9}$$

The forming limit diagram for the EN AW-7108 T6 aluminium alloy is presented in Figure 7.

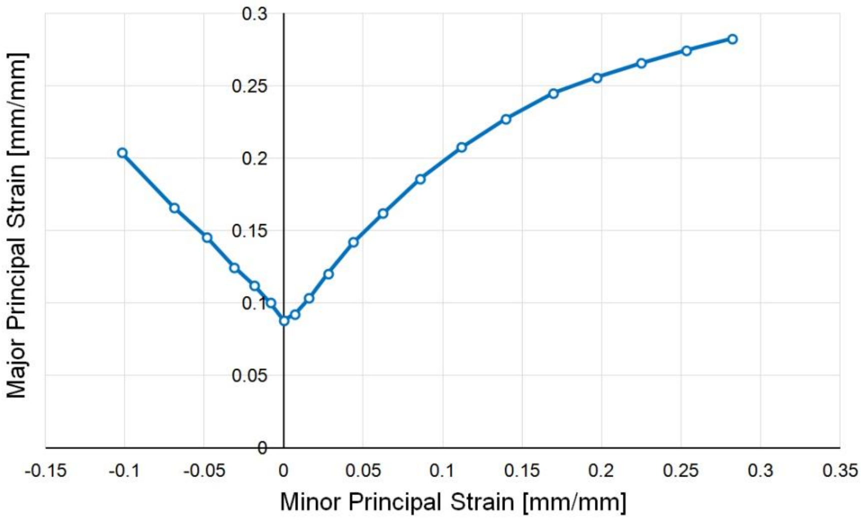

Fig. 7. Variation of the major principal strain with the minor principal strain for the EN AW-7108 T6 aluminium alloy

Numerical Simulations

Model definition

The simulations used in this study to evaluate the described damage initiation criteria consist of a projectile impact at a 45° angle of an extruded aluminium plate with a speed of 50 m/s, the model consisting of a rigid support, a rigid spherical projectile and a shell plate (figure 8). The support was encastred and a general contact with 0.8 friction coefficient was set for the whole model.

The aluminium material model used for the deformable shell plate consisted of an elastic-plastic formulation, having a Young's modulus of $7 \cdot 10^4$ MPa and, a Poisson ratio of 0.33 and a plasticity function (yield stress as a function of plastic strain) described in Figure 9. The stress-strain response of the material model is presented in Figure 10.

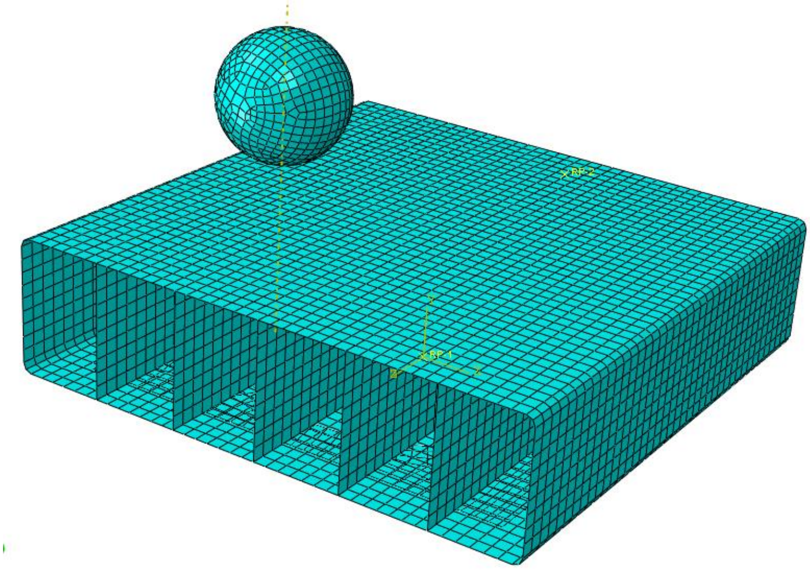

Fig. 8. Angled projectile impact simulation model

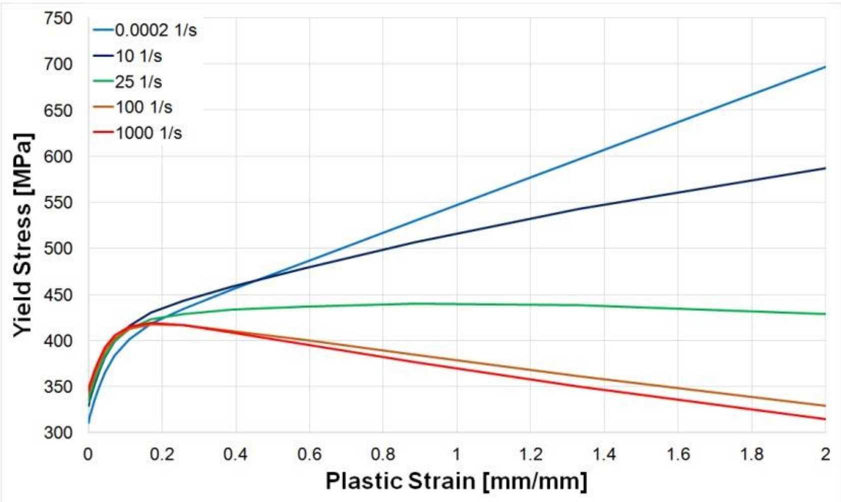

Fig. 9. Yield stress as a function of plastic strain for the EN AW-7108 T6 aluminium alloy model

Simulation results

a) Simulation results for the linear elastic model with no damage. The first simulation was performed on the elastic-plastic material model defined in the previous paragraph, without having any damage initiation criterion implemented. The results for the deformed plate are presented in Figure 11.

b) Simulation results for the Equivalent strains criterion. The second simulation used the elastic-plastic model with the equivalent strains criterion. The deformed model is presented in Figure 12.

c) Simulation results for the Shear criterion. The third simulation used the elastic-plastic model with the shear criterion. The deformed model is presented in Figure 13.

d) Simulation results for the FLD criterion. The third simulation used the elastic-plastic model with the FLD criterion. The deformed model is presented in Figure 14.

e) Simulation results for the combined damage models. The third simulation used the elastic-plastic model with all implemented criteria. The deformed model is presented in Figure 15.

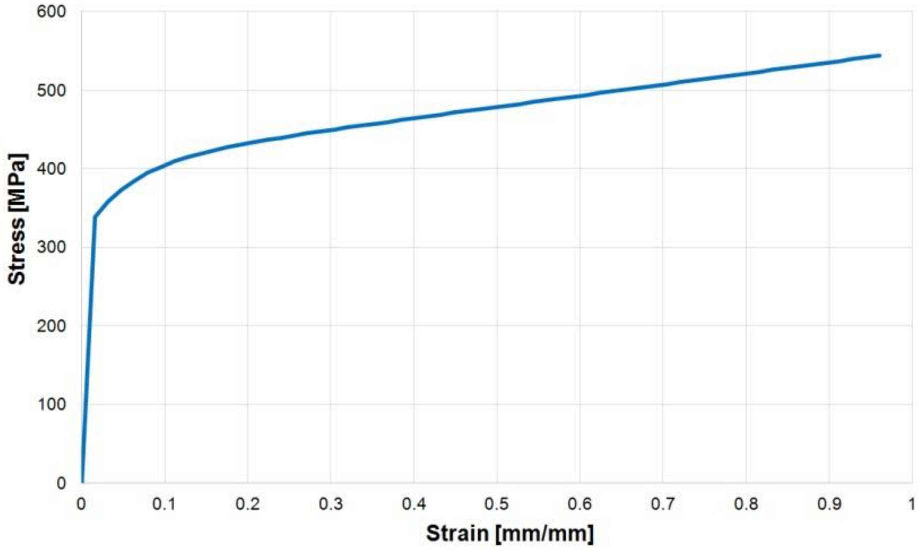

Fig. 10. Stress-strain response of the EN AW-7108 T6 aluminium alloy model

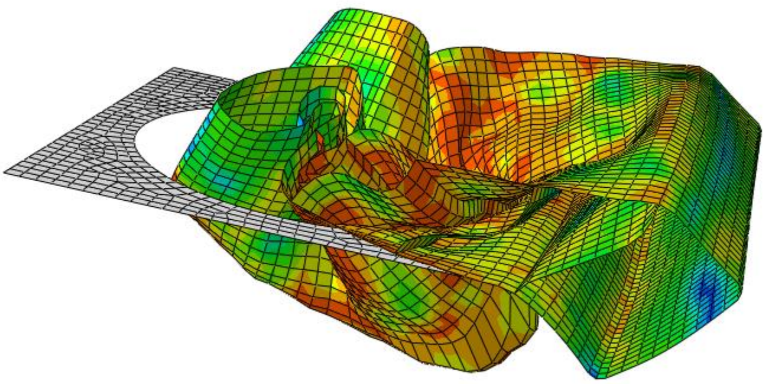

Fig. 11. Deformed model with no damage

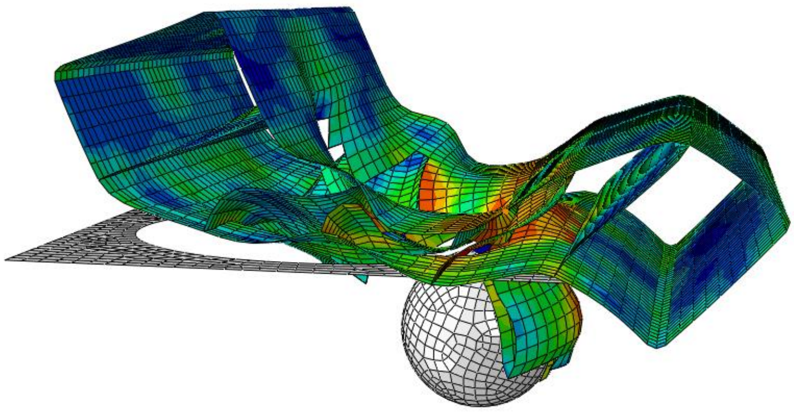

Fig. 12. Deformed model with the equivalent strain criterion

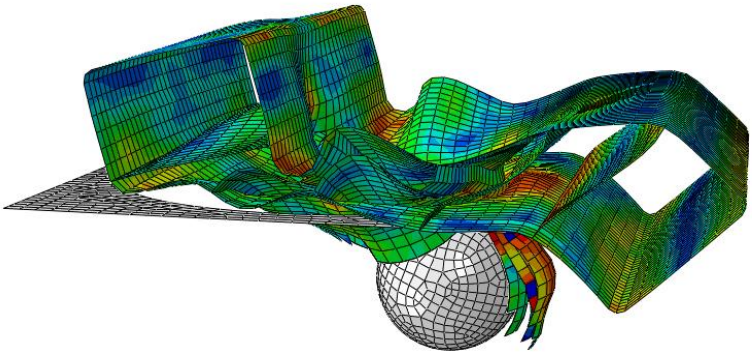

Fig. 13. Deformed model for the shear criterion

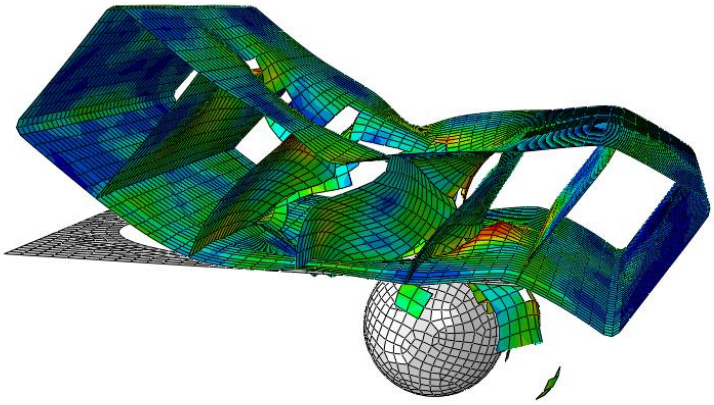

Fig. 14. Deformed model for the FLD criterion

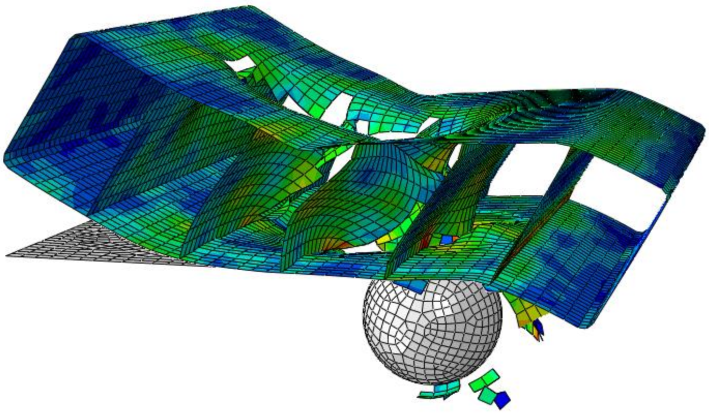

Fig. 15. Deformed model with all damage initiation criteria

Conclusions

This study presents three of the most used damage initiation criteria used in finite element analysis simulations: equivalent strains criterion, shear criterion and the forming limit diagram criterion. Numerical analyses were performed on a projectile impact model, showing the effects of each damage initiation models and the combined effects of all models. It was observed that the model that combined all the damage initiation criteria showed the lowest reaction forces, due to the multiple damage initiation areas determined by each individual criterion.

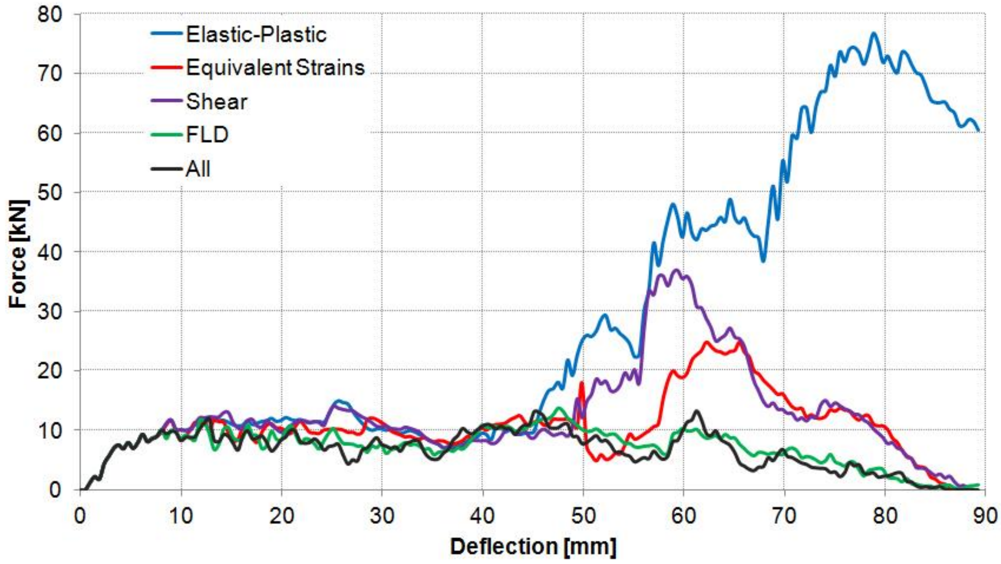

Fig. 16. Reaction-displacement graph for the impact simulations

Acknowledgments

This work was partially supported by the strategic grant POSDRU/159/1.5/S/137070 (2014) of the Ministry of National Education, Romania, co-financed by the European Social Fund – Investing in People, within the Sectoral Operational Programme Human Resources Development 2007-2013 and by the CNCS – UEFISCDI grant PN-II-ID-PCE-2011-3-0456, contract number 172/2011.

References

1. Levanger, H. – *Simulating Ductile Fracture in Steel using the Finite Element Method: Comparison of Two Models for Describing Local Instability due to Ductile Fracture* - Master Thesis. Faculty of Mathematics and Natural Sciences, University of Oslo, 2012.
2. Prant, A., Ruzicka, J., Spaniel, M., Moravec, M., Dzugan, J., Konopík, P. – Identification of Ductile Damage Parameters, *2013 SIMULIA Community Conference*, 2013.
3. Rose, B.D., Yamashita, Y., Anderson, T.L. – FEA Capturing both Brittle and Ductile Crack Propagation, *2010 SIMULIA Customer Conference*, 2005.
4. Leppin, C., Hooputra, H., Werner, H., Weyer, S., Büchi, R.V. – Crashworthiness simulation of aluminium pressure die casting including fracture prediction, *International Conference on Computational Plasticity*, 2005.
5. Abaqus – *User's Manual*, vol. *Analysis*, 2011.
6. Wierzbicki, T., Bao, Y., Lee, Y.W., Bai, Y. – Calibration and evaluation of seven fracture models, *International Journal of Mechanical Sciences*, Vol. 45, 2005, pp. 719–743.
7. Bonora, N. – On the effect of triaxial state of stress on ductility using nonlinear CDM model, *International Journal of Fracture*, Vol. 88, 1997, pp. 359–371.
8. Mirone, G. – Role of stress triaxiality in elastoplastic characterization and ductile failure prediction, *Engineering Fracture Mechanics*, Vol. 74, 2007, pp. 1203–1221.
9. Bonora, N., Gentile, D., Pirondi, A., Newazc, G. – Ductile damage evolution under triaxial state of stress: theory and experiments, *International Journal of Plasticity*, Vol. 21, 2005, pp. 981–1007.
10. Bao, Y., Wierzbicki, T. – On the cut-off value of negative triaxiality for fracture, *Engineering Fracture Mechanics*, Vol. 72, 2005, pp. 1049–1069.

11. Bao, Y., Wierzbicki, T. – On fracture locus in the equivalent strain and stress triaxiality space, *International Journal of Mechanical Sciences*, Vol. 46, 2004, pp. 81–98.
12. Bao, Y. – Dependence of ductile crack formation in tensile tests on stress triaxiality, stress and strain ratios, *Engineering Fracture Mechanics*, Vol. 72, 2005, pp. 505–522.
13. Hooputra, H., Gese, H., Dell, H., Werner, H. – A comprehensive failure model for crashworthiness simulation of aluminium extrusions, *International Journal of Crashworthiness*, Vol. 9, No. 5, 2004, pp. 449-464.
14. Hogström, P., Ringsberg, J.W., Johnson, E. – Experimental verification of finite element failure criteria with respect to strain state and element size, *Proceedings of the Twelfth International Conference on Fracture*, 2009.

Modelarea numerică a degradării și ruperii materialelor ductile în analiza cu elemente finite

Rezumat

În această lucrare sunt expuse principalele modele numerice folosite la simularea degradării şi ruperii materialelor ductile, implementate în unele pachete software de simulare cu elemente finite: criteriul deformațiilor echivalente, criteriul deformațiilor tangențiale, criteriul FLD și MSFLD. Au fost efectuate simulări pentru o solicitare dinamică folosind câte unul din criteriile prezentate precum și un model cu toate criteriile, observându-se efectul fiecărui criteriu asupra modulul de cedare al piesei.